Bull. Fac. Fish. Hokkaido Univ.
26(3), 235–248. 1975.

Spectral Distribution of Underwater Irradiance

Kichiichiro KAWANA*

Abstract

The spectral distributions in the sea near Hakodate in Hokkaido are obtained by an irradiance meter with the calibrations of the absolute spectral response and the immersion effect correction.

As for the measured results of the downward underwater irradiance, the spectral distribution in the surface layer is asymmetric and the peak energy is observed near 500 mμ. As depth increases, the longer wave light more than 600 mμ decreases rapidly and the peak shifts slowly towards the shorter wavelength. The spectral distribution of the upward irradiance is symmetric even in the surface layer. The peak of energy is observed at a shorter wavelength rather than the downward irradiance.

The theoretical downward irradiance is calculated on the basis of Kishino's method. Theoretical results agree well with the measured values at every water depth.

Introduction

Light distribution in the sea depends on both attenuation and scattering processes, namely inherent optical properties of sea water, which are variable due to the selective absorption of water and also to the suspended materials in the sea. In other words, light intensity in the sea is influenced considerably by the wavelength and the turbidity of sea water. To explain such light in nature in detail, several authors attempted to design an apparatus for measuring the spectral irradiance. Sasaki et al.[1] designed an irradiance meter which consisted in a photomultiplier tube and six colour filters. Jerlov[2] measured the spectral irradiance by a new type meter in which eight interference filters were set. Tyler and Smith[3] designed an underwater spectroradiometer and they performed measurements in the Crater Lake and various oceans.[4] Sasaki et al.[5] and Kishino et al.[6] measured the irradiance, scalar irradiance and attenuation coefficient in the adjacent region of the Kuroshio and discussed the optical properties of sea water.

The present author measured the spectral distribution of irradiance near Hakodate in Hokkaido by a specially designed irradiance meter. The optical system of the irradiance meter and the error of the cosine collector were discussed in a previous paper.[7] In this paper the calibration of absolute radiant energy and the immersion effect are explained and the theoretical downward irradiance including up to the multiple order scattering is calculated on the basis of Kishino's

* *Research Institute of North Pacific Fisheries, Hokkaido University*
(北海道大学水産学部北洋水産研究施設)
Present: *Goverment Industrial Research Institute, Chugoku* (現在: 中国工業技術試験所)

method.[8] In the calculation, measured values are used for inherent optical properties. The theoretical treatment and the comparison of the calculated results with the measured values are discussed.

Calibration of the irradiance meter

The irradiance meter in this paper has seven interference filters, of which characteristic curves in regard to wavelength are shown in Fig. 1.

Lighting up vertically with a halogen lamp, the absolute response of the irradiance meter is calibrated by measuring the irradiance from the horizontal direction. The absolute value of the radiant energy is obtained easily by changing the distance between the lamp and the collector of the irradiance meter and applying the inverse-square law of the distance. An example of the relationship between the reading of meter and the radiant energy for the wavelength of 503 mμ is shown in Fig. 2. The solid line is obtained by the least square method. The gradient of the line is a correction of the radiant energy for 503 mμ. Correction values for various wavelengths are summerized in Table 1.

When the irradiance meter is submerged in the sea, a large percentage of the incident radiant flux is more back-scattered into the water than into the air due to the change of the refraction index at the interface of the collector. This phenomenon is called *the immersion effect.* As described above, the absolute spectral response of the irradiance meter in the experiment is obtained in the air,

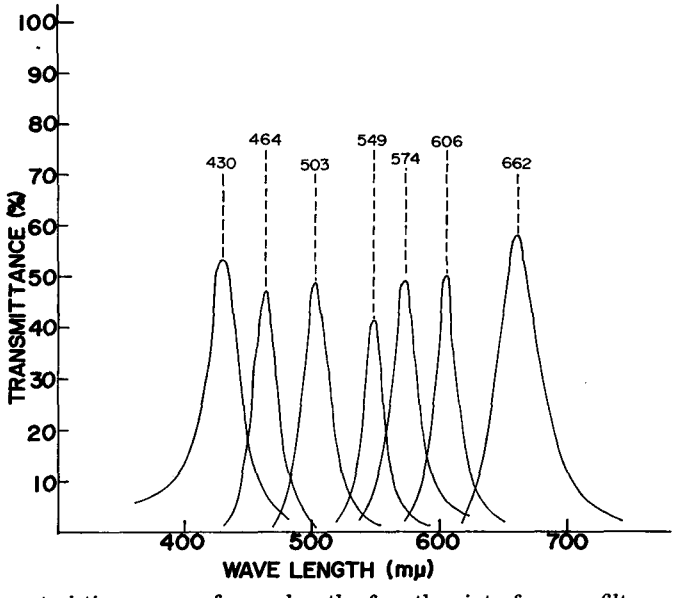

Fig. 1. Characteristic curves of wavelength for the interference filter used in the irradiance meter.

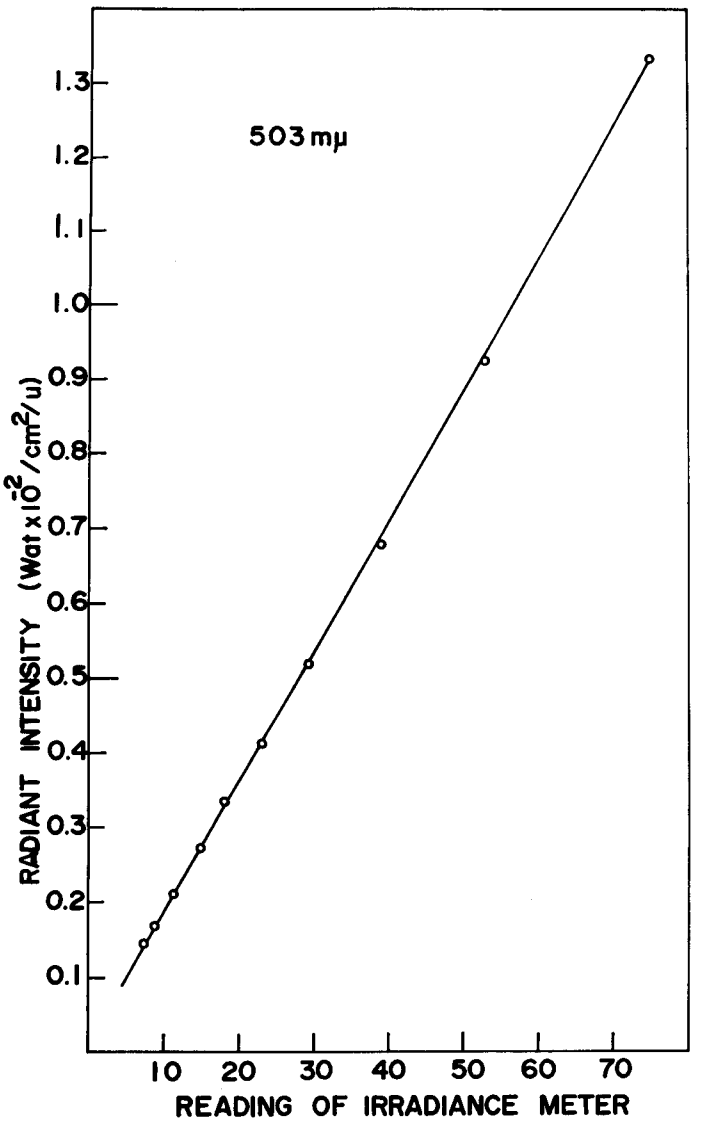

Fig. 2. Calibration curve of the radiant energy and the recorder reading of the irradiance meter at 503 mμ.

thus it is necessary to make a correction for the immersion effect in the water. The method to calibrate the immersion effect for the irradiance meter is carried out by the same way as Smith[9]. The irradiance meter is suspended into the water tank blackened inside and a steady collimated beam of radiant energy is directed perpendicularly upon the collector of the irradiance meter. The

Table 1. The collection values of the radiant energy and the recorder reading of irradiance meter. (Wat $\times$ 10^{-5}/cm^2=Reading$\times$G)

Wavelength (mμ)	G
430	8.263
464	15.976
503	17.741
549	50.817
574	44.624
606	94.264
662	116.656

schematic diagram of the experiment is shown in Fig. 3. The response of the irradiance meter is measured for the case of several water depths and the air. The ratio of the response in the water ($V_W(z)$) to that in the air (V_a) is plotted in Fig. 4. The solid line is yielded by the least square method. By extrapolating the line to zero depth, the value of the response in the water at zero depth (V_W') can be estimated. The energy loss at the air-water interface is calculated by using the Frensnel equation. For normal incidence, the transmittance (T) at the air-water interface is expressed thus:

$$T = 1-(n-1)^2/(n+1)^2$$

where n is the refractive index of water relative to the air. The correction

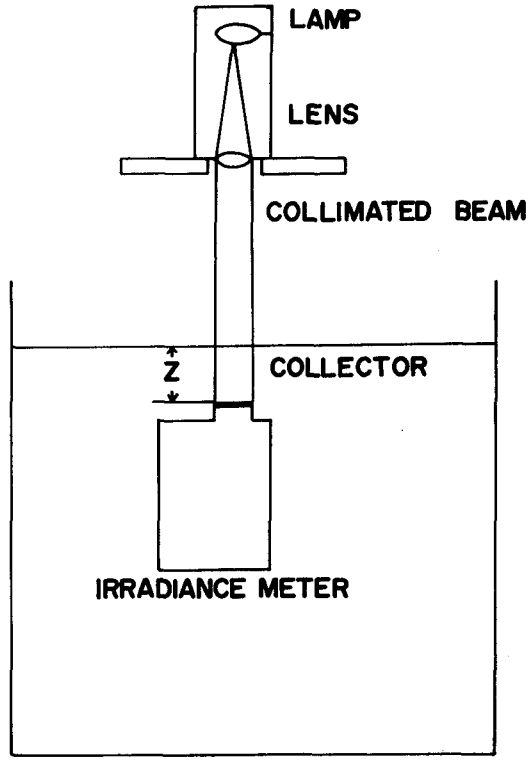

Fig. 3. Experimental arrangement used to measure the immersion effect correction.

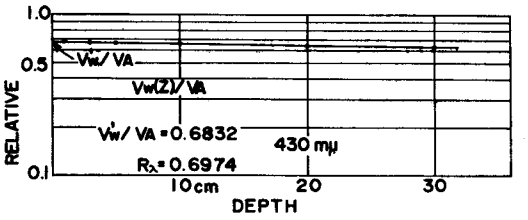

Fig. 4. The response of the irradiance collector in underwater divided by its response in air versus the depth of water above the collector's surface. V_W'/V_A is the zero depth intercept calculated from the least-squares method.

Table 2. The correction values of the spectral immersion effect.

Wavelength (mμ)	R
430	0.6974
464	0.7008
503	0.7053
549	0.7104
574	0.7258
606	0.7261
662	0.7273

value (R_λ) due to the *immersion effect* is given by the following equation:

$$R_\lambda = (V_W'/V_A) \cdot (1/T)$$

The results of correction value for each wavelength are summerized in Table 2. The absolute radiant energy can be obtained by multiplying the reading of irradiance meter with a correction value for the radiant energy and a reciprocal R for the *immersion effect.*

Results and Discussion

The spectral curves of downward and upward irradiances near Hakodate are shown in Fig. 5, Fig. 6 and Fig. 7. The solid lines show the downward irradiances and the dotted lines the upward irradiances. The numerical values in the figure are the depth from the surface. Fig. 5 shows the result obtained at the Funka Bay (42°04'N, 141°09'E) for solar altitude of 32°15'. Fig. 6 is the spectral distribution at the Tsugaru Straits (41°16'N, 140°26'E) for solar altitude of 21°26', and Fig. 7 is off Hakodate Bay (41°42'N, 140°43'E) on the overcast.

In a clear sky, the total radiant flux arrived just above the sea surface consists of the direct sun light and the scattered light. According to Judd,[10] the spectral distribution of the total radiant flux measured between 350 mμ and 800 mμ of the wavelength was unrelated to the solar altitude, when it was within the range from 15° to 90°. However when the solar altitude decreased less than about 15°, the spectral distribution differed considerably from the high solar altitude. For the high solar altitude, there was a peak of the total radiant flux in the range from 480 mμ to 520 mμ and moreover the spectral distribution was asymmetric. On the other hand, the total radiant flux in the overcast time of the scattered sun light arrived at the sea surface was asymmetric and the peak energy was seen near 500 mμ.

In our experimental results, it is recognized from the downward irradiance that the spectral distributions in the surface layer are asymmetric and the peak energy is observed in the range of 500 mμ to 550 mμ. The peak may be unrelated

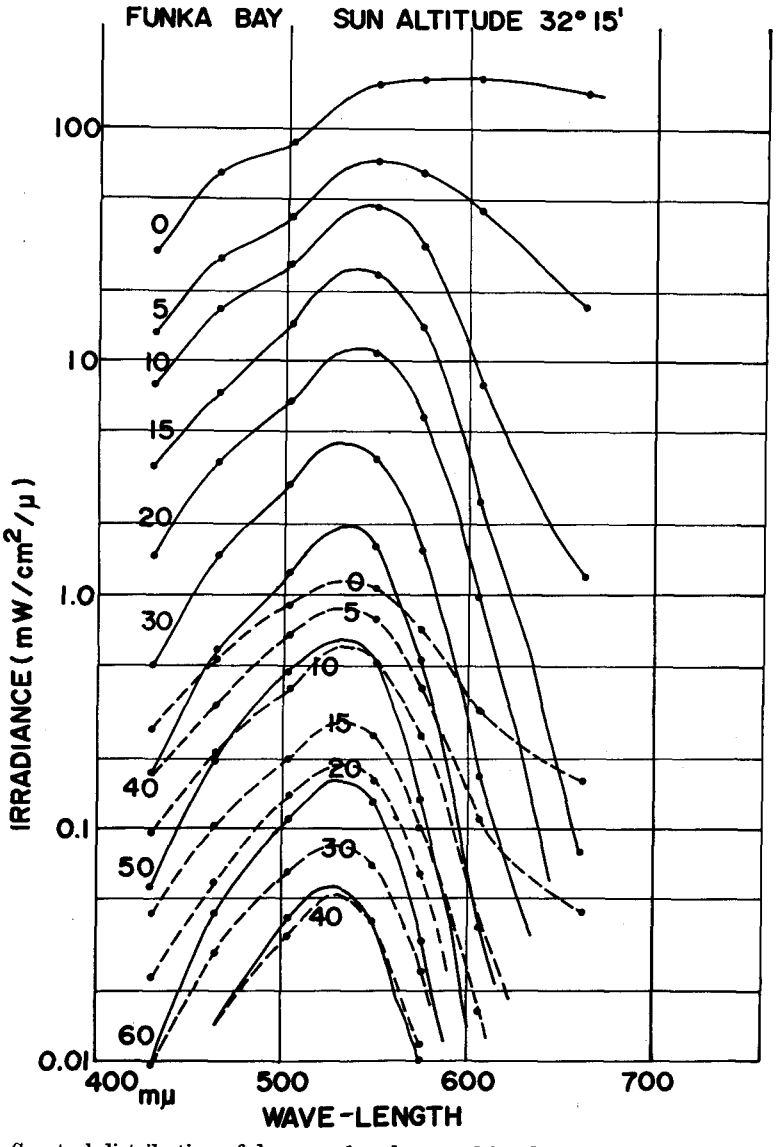

Fig. 5. Spectral distribution of downward and upward irradiance at Funka Bay (42°04′N, 141°09′E) for solar altitude of 32°15′.

to the solar altitude, because the spectral distribution above the sea surface is almost the same with the solar altitude. With increasing depth, the longer wave light of more than 600 mμ decreases rapidly and the peak of energy shifts slowly towards the shorter wavelength. Thus the spectral distribution becomes symmetric

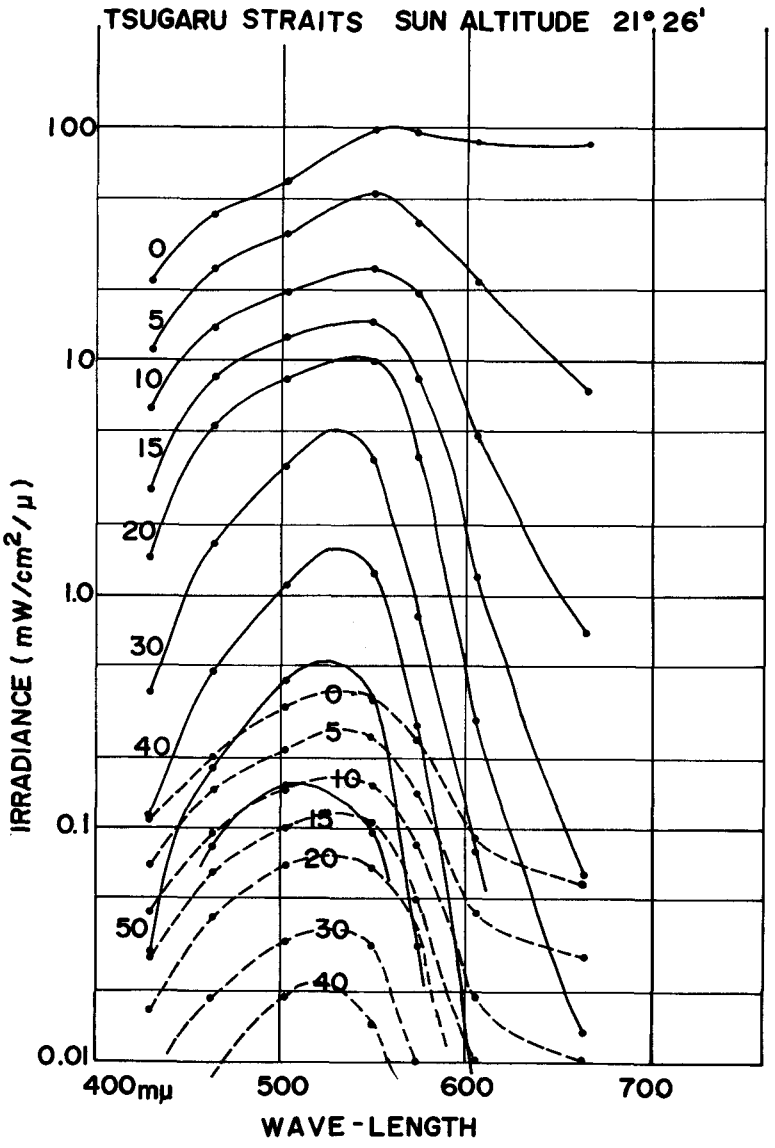

Fig. 6. Spectral distribution of downward and upward irradiance at Tsugaru Straits (41° 16'N, 140°26'E) for solar altitude of 21°26'.

and as to the light in the deeper layer, only the monochromatic light remains.

The spectral distributions of the upward irradiance are symmetric even in the surface layer and the peak of energy is better observed at the shorter wavelength than the peak of the downward irradiance. The reason is that the

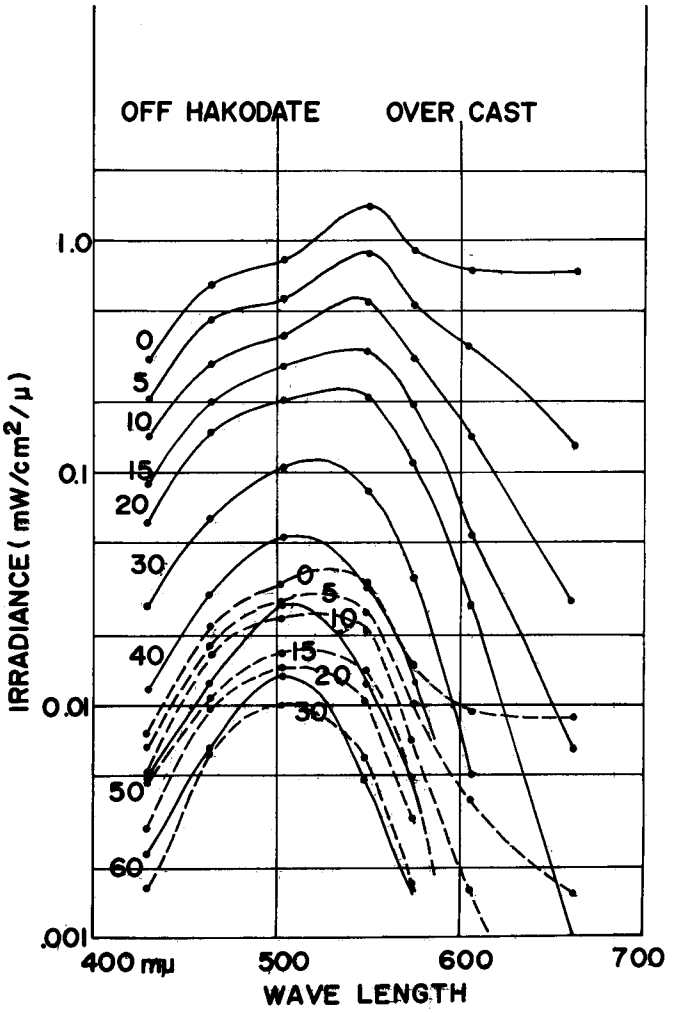

Fig. 7. Spectral distribution of downward and upward irradiance off Hakodate Bay (41°42′N, 140°26′E) on the overcast.

upward irradiance is composed of the multiple scattered light which is propagated from the deep layer toward the sea surface. As is evident from the spectral distribution of the downward irradiance, the remained light in the deep layer consists of a wavelength of 480 mμ to 550 mμ. Since this light influences upon the upward irradiance in the surface layer, the peak tends to appear at the shorter wavelength with increasing depth and finally agrees with the peak of the downward irradiance in the deep layer.

The transmittance of the irradiance in the sea depends on the wavelength of light and the turbidity of sea water. In order to classify the ocean water,

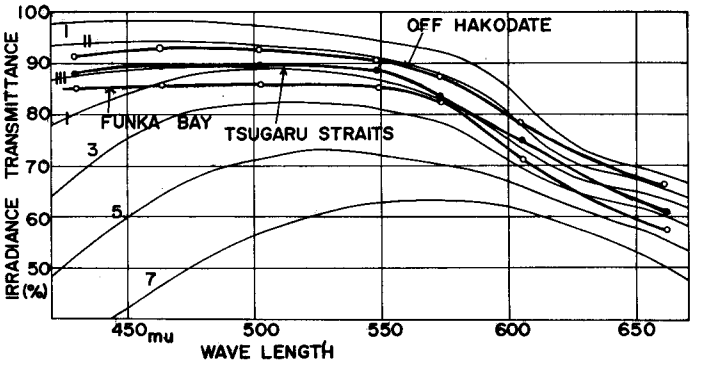

Fig. 8. Spectral transmittance per meter of downward irradiance at Funka Bay, Tsugaru Straits and off Hakodate Bay. I, II and III in the figure show the oceanic types for optical classification of Jerlov and 1, 3, 5 and 7 show coastal types.

Jerlov[11] proposed the method of optical classification of ocean water in regard to the type of spectral transmittance of downward irradiance at high solar altitude. That is, as for the ocean water, he represented three water types referring to the normal transmittance curves in surface waters and as for the coastal waters, he classified into 9 types from observation along the coast of Scandinavia and Western North America. The comparison between the measured values with Jerlov's classification is shown in Fig. 8. The transmittance is the average of the water column between 0 m and 50 m, and 1, 11 and 111 in the figure show the oceanic types proposed by Jerlov. As seen clearly from the figure, the Tsugaru Straits is ocean type-111 and the water of the Hakodate Bay is type-11.

Theoretical treatment: The light energy penetrated into the sea is absorbed and scattered by water molecules and suspended particles which influence upon the distribution of underwater irradiance. The process of scattering in the sea is very complicated. Theoretical treatments of the light transfer in the sea have been examined by many investigators (Schuster[12], Jerlov[13], Preisendorfer[14]) and recently, Kishino[8] proposed a simple model which was a pile of single scattering layers and explained the radiation field in the ocean. In this paper, the theoretical downward irradiance is calculated by the same method as in Kishino's.

The incident light penetrated into the sea through the sea surface is composed of both the direct sun light and the scattered sky light. The direct sun light is once refracted at the sea surface and enters in a direction which depends upon the incident direction. The scattered sky light entering the sea is diffused downward in all directions. In the following treatment, however, it is assumed that the scattered light is diffused only in the vertical direction and the sea consists of a pile of very thin parallel layers as shown in Fig. 9. Moreover, it is assumed that only the first order scattering takes place in each layer. The scattered light in the sea due to the scattered sky light is estimated as well as the direct sun light.

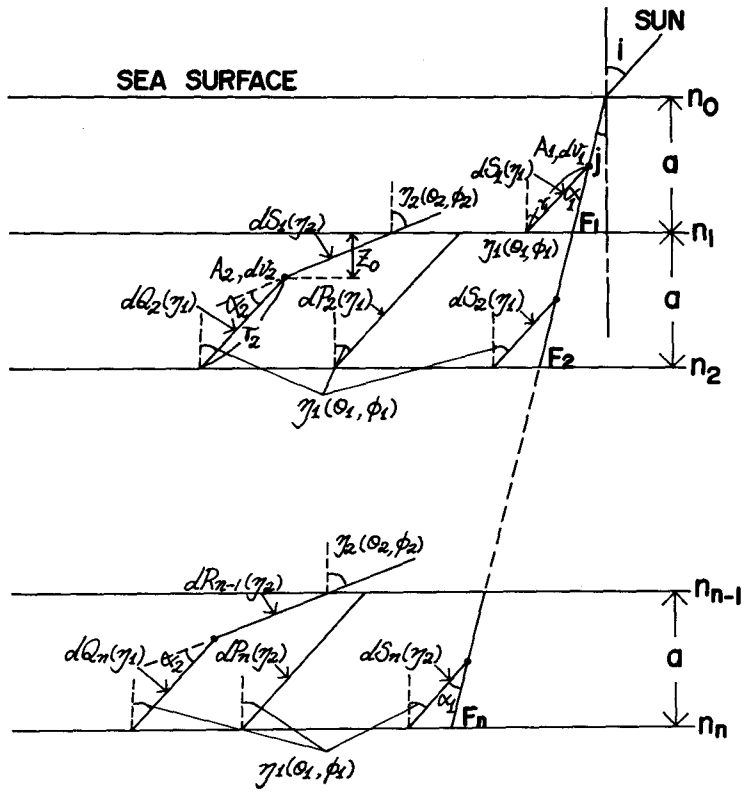

Fig. 9. Schematic diagram showing the irradiance up to the multiple scattering.

a. The first layer

The direct sun light entering the first layer is scattered at a point A_1 in the direction (θ_1, ϕ_1), where θ_1 is a vertical angle and ϕ_1 is a horizontal angle. The direction $(\theta_1\ \phi_1)$ and the first order scattered light are denoted as η_1 and $dS_1(\eta_1)$. The downward irradiance E_1 at n_1 is as follows:

$$E_1 = F_1 + \int_0^{\Omega} \cos\theta_1 \cdot dS_1(\eta_1) \tag{1}$$

where F_1 is the direct attenuated sun light and stands for integration of over the upper hemisphere. F_1 and $dS_1(\eta_1)$ are expressed as follows respectively:

$$F_1 = E_0 e^{-c_1 \cdot a \cdot \sec j} \tag{2}$$

$$dS_1(\eta_1) = E_0 \cdot \sec j \cdot \sec\theta_1 \cdot \beta_1(\alpha_1) \cdot \frac{e^{-c_1 \sec j \cdot a} - e^{-c_1 \cdot \sec\theta_1 \cdot a}}{c_1(\sec\theta_1 - \sec j)} \sin\theta_1 \cdot d\theta_1 \cdot d\phi_1 \tag{3}$$

where E_0 is the downward irradiance at the sea surface, c_1 the beam attenuation

coefficient of the first layer at the thickness of layer, $\beta(\alpha_1)$ the volume scattering function and α_1 an angle between the incident beam and the direction (θ_1, ϕ_1). Eq. (1) is integrated with respect to θ_1 from 0 to $\pi/2$ and ϕ_1 from 0 to 2π.

b. The second layer

In the second layer, incident lights from the first layer are assumed to consist of the direct attenuated light F_1 and the scattered light $dS_1(\eta_1)$. F_1 yields the direct attenuated light F_2, and the scattered light $dS_2(\eta_1)$ and $dS_1(\eta_1)$ yield the attenuated light $dP_2(\eta_1)$ and the secondary scattered light $dQ_2(\eta_1)$. Though $dS_1(\eta_1)$ enters from all directions, the direction of $dS_1(\eta_1)$ in the second layer is denoted as $\eta_2(\theta_2, \phi_2)$. The light $dS_1(\eta_2)$ from the direction $\eta_2(\theta_2, \phi_2)$ is scattered at point A_2 in the direction $\eta_1(\theta_1, \phi_1)$. An angle between $\eta_1(\theta_1\ \phi_1)$ and $\eta_2(\theta_2, \phi_2)$ is expressed as α_2. All the scattered light $dR_2(\eta_1)$ in the direction $\eta_1(\theta_1, \phi_1)$ at n_2 is the sum of $dS_1(\eta_1)$, $dP_2(\eta_1)$ and $dQ_2(\eta_1)$. The downward irradiance E_2 at n_2 is obtained as follows:

$$E_2 = F_2 + \int_0^{\Omega} \cos\theta_1 \cdot dR_2(\eta_1) \tag{4}$$

where Ω stands for the integration of $dR_2(\eta_1)$ over the upper hemisphere. F_2, $dS_2(\eta_1)$, $dP_2(\eta_1)$ and $dQ_2(\eta_1)$ are obtained as follows respectively:

$$F_2 = F_1 \cdot e^{-c_2 \cdot a \cdot \sec j}$$

$$dS_2(\eta_1) = F_1 \cdot \sec j \cdot \sec\theta_1 \cdot \beta_2(\alpha_1) \frac{e^{-c_2 \cdot \sec j \cdot a} - e^{-c_2 \cdot \sec\theta_1 \cdot a}}{c_2(\sec\theta_1 - \sec j)} \sin\theta_1 \cdot d\theta_1 \cdot d\phi_1 \tag{6}$$

$$dP_2(\eta_1) = dS_1(\eta_1) \cdot e^{-c_2 \cdot \sec\theta_1 \cdot a} \tag{7}$$

$$dQ_2(\eta_1) = \left\{ \int_0^{2\pi} \int_0^{\pi/2} \cdot \beta_2(\alpha_2) \frac{e^{-c_2 \cdot \sec\theta_2 \cdot a} - e^{-c_2 \cdot \sec\theta_1 \cdot a}}{c_2(\sec\theta_1 - \sec j)} dS_1(\eta_2) \right\} \sec\theta_1 \cdot \sin\theta_1 \cdot d\theta_1 \cdot d\phi_1 \tag{8}$$

$$dR_2(\eta_1) = dS_2(\eta_1) + dP_2(\eta_1) + dQ_2(\eta_1) \tag{9}$$

c. The n-th layer

According to the model described above, the light entering the n-th layer can be expressed as F_{n-1} and $dR_{n-1}(\eta_1)$. The attenuated light F_n and the scattered light $dS_n(\eta_1)$ originated from F_{n-1} are obtained by the same way in the second layer. $dP_n(\eta_1)$ and $dQ_n(\eta_1)$ originated from $dR_{n-1}(\eta_1)$ are obtained by replacing $dS_1(\eta_1)$ in the second layer with $dR_{n-1}(\eta_1)$. The total scattered light $dR_n(\eta_1)$ in the direction $\eta_1(\theta_1, \phi_1)$ at n_n is the sum of $dS_1(\eta_1)$, $dP_n(\eta_1)$ and $dQ_n(\eta_1)$. The downward irradiance E_n at n_n is given as follows:

$$E_n = F_n + \int_0^{\Omega} \cos\theta_1 \cdot dR_n(\eta_1) \tag{10}$$

where Ω implies the integration of $dR_n(\eta_1)$ over the hemisphere.

Comparison of the experimental results with the theoretical results: In the calculation, both the beam attenuation coefficients and volume scattering functions are assumed to be a constant from the sea surface to the deep layer and the thickness of the layer is assumed as one meter.

The calculation is performed by using the computer as follows. The first order scattered light $dS_1(\eta_1)$ in the first layer is calculated from Eq. (3) at intervals of 10° for θ and ϕ. These results are stored in the computer. Next, the scattered light $dS_2(\eta_1)$ in the second layer is calculated in the same manner. Based on the previously memorized $dS_1(\eta_1)$, the attenuated light $dP_2(\eta_1)$ and the secondary scattered light $dQ_2(\eta_1)$ are calculated from Eq. (7) and Eq. (8) respectively. Using $dS_2(\eta_1)$, $dP_2(\eta_1)$ and $dQ_2(\eta_1)$, the total scattered light $dR_2(\eta_1)$ at depth n_2 is obtained easily from Eq. (9). The procedure is performed repeatedly at the given depth. The theoretical downward irradiance E_n at depth n_n is calculated from Eq. (10) by the numerical integration.

Calculations are carried out to the wavelengths 436 mμ and 546 mμ. The volume scattering functions used in the calculations are measured *in situ*. Theoretical results for the Tsugaru Straits and off Hakodate are shown in Fig. 10

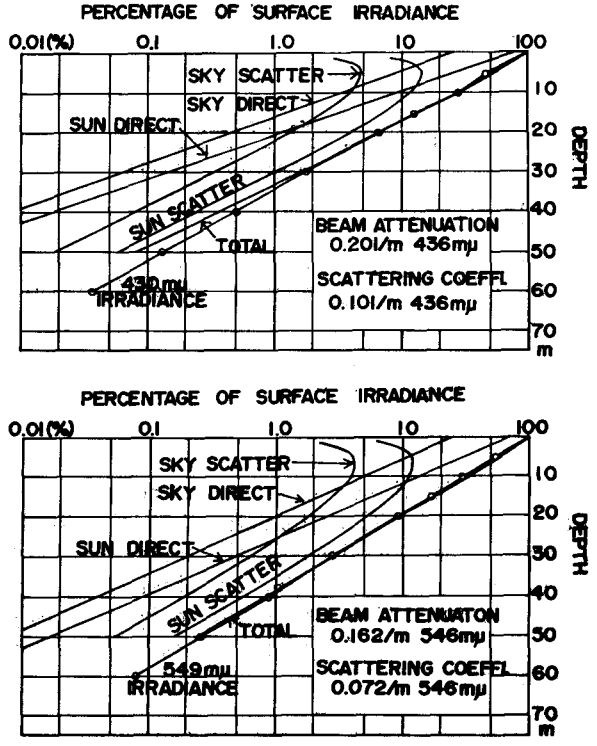

Fig. 10. Comparisons of the measured irradiance at Tsugaru Straits with theoretical result.

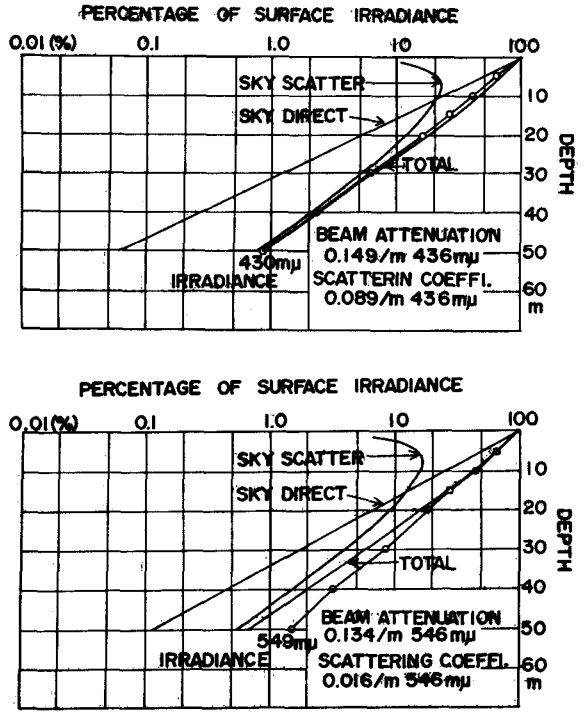

Fig. 11. Comparisons of the measured irradiance off Hakodate Bay with theoretical result.

and Fig. 11. In the figures, the direct attenuated sun light F_n is expressed as *SUN DIRECT* and the multiple scattered light R_n as sun light *SUN SCATTER*. *SKY DIRECT* and *SKY SCATTER* show the attenuated light for the scattered sky light and the multiple scattered light respectively. *TOTAL* means the theoretical downward irradiance E_n and *IRRADIANCE* is the experimental result measured *in situ*. Numerical values of the volume scattering function and the beam attenuation coefficient are expressed in the figures. In Fig. 11, being measured at the overcast, the incident light entering the sea is assumed to be only the scattered sky light.

As is clear from Fig. 10 and Fig. 11, the multiple scattered light has a maximum at a few meters from the sea surface. The direct attenuated light is larger than the multiple scattered light close to the sea surface. With the increasing of the depth, however, the multiple scattered light becomes larger than the direct attenuated light. The difference between both values tends to increase with the depth.

The theoretical downward irradiance agrees well with the measured values at every water depth. However in some case, it appears that the theoretical results in deep layer are smaller than the experimental results. If the thickness of the

layer estimated in the calculation is smaller than one meter, a close agreement between the theoretical and experimental result will be expected.

Acknowledgements

The author would like to acknowledge the continuing guidance and encouragement of Emeritus Professor Naoichi INOUE of Hokkaido University and also thank Professor Masami ISHIDA and Professor Rihei KAWASHIMA of Hokkaido University for their helpful advice. The author also wishes to thank Associate Professor Masahiro KAJIHARA and the staff of the Research Institute of North Pacific Fisheries, Faculty of Fisheries, Hokkaido University for their helpful advice.

References

1) Sasaki, T., Okami, N., Watanabe, S. and Oshiba, G. (1955). Measurements of the angular distribution of submarine daylight. *J. Sic. Res. Inst.* **49**, 103–106.
2) Jerlov, N.G. (1965). Optical studies of ocean water. *Rept. Swedish Deep-Sea Expedition* **3**, 73–97.
3) Tyler, J.E. and Smith, R.C. (1966). Submersible spectroradiometer. *J. Opt. Soc. Amer.* **56**, 1390–1396.
4) Tyler, J.E. and Smith, R.C. (1970). Measurements of spectral irradiance underwater. *Gordon and Breach* 103p.
5) Sasaki, T., Okami, N., Kishino, M. and Oshiba, G. (1968). Optical properties of the water in adjacent region of the Kuroshio. *J. Oceanog. Soc. Japan* **24**, 45–50.
6) Kishino, M., Okami, N., Oshiba, G. and Sasaki, T. (1972). Optical properties of the water in adjacent region of the Kuroshio II. *La mer.* **10**, 89–94.
7) Kawana, K. (1972). Effect of the scattered light on underwater irradiance. *Bull. Fac. Fish. Hokkaido Univ.* **23**, 82–93.
8) Kishino, M. (1974). Numerical Calculation of Radiative Transfer in the Sea. *La mer.* **12**, 26–33.
9) Smith, R.C. (1969). An underwater spectral irradiance collector. *J. Mar. Res.* **27**, 341–351.
10) Judd, D.B., McAdam, D.L. and Wysjecki, G. (1964). Spectral distribution of typical daylight as a function of corrected colour temperature. *J. Opt. Soc. Amer.* **54**, 1031– 1040.
11) Jerlov, N.G. (1968). Optical Oceanogrphy. *Elsevier Oceanogr. Ser.* **5**, 194p.
12) Schuster, A. (1905). Radiation through a foggy atmosphere. *Astrophys. J.* **21**, 1–22.
13) Jerlov, N.G. and Fukuda, M. (1960). Radiation distribution in the upper layer of the sea. *Tellus* **12**, 348–355.
14) Preisendorfer, R.W. (1964). Physical aspect of light in the sea. *Univ. Hawai. Press. Honolulu Hawaii* 51–60.